EARTH AND PLANETARY SCIENCE LETTERS 18 (1973) 125–132. NORTH-HOLLAND PUBLISHING COMPANY

ON THE EQUATIONS OF STATE OF HIGH-PRESSURE SOLID PHASES

Dae H. CHUNG
Weston Observatory, Boston College, Weston, Massachusetts 02193

Received 3 October 1972
Revised version received 17 November 1972

A practical scheme by which one can construct equations of state of high-pressure solid phases that cannot be determined experimentally given the present state of technology, is proposed and illustrated with three examples for its possible application to the study of elasticity and the constitution of the earth's mantle.

1. Introduction

Most of the known mantle minerals found at ambient conditions undergo one or more phase changes in the pressure and temperature field of the earth's interior. Finding the proper equations of state of solids before and after a phase change is essential in the interpretation of geophysical field observations as well as in our understanding of solid-state properties of these materials. The bulk modulus K and its first derivative with respect to pressure (dK/dp) are the important parameters entering into equations describing the pressure-volume relationship of the solid [1]. Laboratory measurements of these equation-of-state (EOS) parameters for solid phases found at ambient conditions are now routine procedures in most ultrasonic-pressure laboratories. For solid phases that exist at high pressures, however, such measurements cannot be made given the present state of technology. The purpose of this communication is to suggest a practical scheme by which one can estimate values of these EOS parameters of high-pressure phases and then to illustrate the scheme with three examples.

2. Scheme

Using Birch's law [2] to estimate velocities of elastic waves in a mineral undergoing compression is now well-known [3, 4]. Chung [3] using Birch's law, has also estimated velocities of compressional (V_p), shear (V_s) and bulk (V_ϕ) waves in the olivine-transformed spinels. Since the adiabatic bulk modulus K_s is related to density ρ and the bulk sound velocity V_ϕ as

$$K_s = \rho\, V_\phi^2, \tag{1}$$

the K_s value of a solid phase after the phase change can be found. (It is noted that $K_s = K\,(1 + T\alpha\gamma)$, where α is the coefficient of volume expansion, γ Grüneisen's ratio and T the temperature in degrees Kelvin, and that the value of this isothermal bulk modulus K is smaller than that of K_s by a few percent in general.) Thus, the first of the two EOS parameters is found for high-pressure phases in this rather straightforward manner.

The second EOS parameter to be found is (dK/dp), which cannot be measured ultrasonically given the present state of technology. It is for this parameter that the author suggests an approximation scheme whereby one can estimate values of $(\partial K_s/\partial p)$ for high-pressure phases.

Recall Birch's law for V_ϕ [4]:

$$V_\phi = a\,(\bar{m}) + b\rho, \tag{2}$$

where $\bar{m}$ is the mean atomic weight and the constants a and b are obtainable from a least-squares fit of experimental values of V_ϕ for substances of similar $\bar{m}$ or for substances of the same $\bar{m}$ as illustrated with periclase by Wang [4]. In view of eqs. (1) and (2), the adiabatic bulk modulus K_s is

$$K_s = \rho\,(a + b\rho)^2. \tag{3}$$

Table 1
Elasticity data of some minerals and rocks with mean atomic weight of 20 to 21.

	$\bar{m}$	ρ (g/cm^3)	V_p (km/sec)	V_ϕ	K_S (mb)	Calculated $\left(\frac{\partial K_S}{\partial p}\right)_S$ Eq. (4)	Calculated $\left(\frac{\partial K_S}{\partial p}\right)_S$ Eq. (5)	Measured $\left(\frac{\partial K_S}{\partial p}\right)_T$
rly	21.0	2.674	6.23	4.63	0.573	4.1	5.8	–
rly	21.0	2.672	6.45	4.61	0.568	4.1	5.9	–
ort	21.6	2.678	6.51	4.81	0.620	4.0	5.6	–
Mt.	20.7	2.679	6.40	4.63	0.574	4.1	5.8	–
	20.8	2.708	6.39	4.72	0.603	4.0	5.7	–
ır	20.2	2.694	6.76	5.01	0.676	3.9	5.4	–
	20.4	3.223	8.28	6.11	1.203	3.8	4.6	–
er	21.0	3.287	7.78	5.87	1.133	4.0	4.9	–
	20.9	3.346	8.28	6.29	1.324	3.8	4.6	–
	20.9	3.312	8.42	6.31	1.320	3.8	4.6	–
	21.0	3.340	7.820	5.607	1.050	4.2	5.2	–
	21.0	3.380	7.850	5.499	1.022	4.3	5.3	–
	20.1	3.224	8.569	6.316	1.286	3.7	4.5	5.37
	20.1	3.222	8.593	6.330	1.291	3.7	4.5	4.97
	20.1	3.217	8.534	6.309	1.281	3.7	4.5	5.04
pc	20.6	3.273	8.422	6.245	1.277	3.8	4.6	5.08
sc	20.7	3.311	8.421	6.252	1.294	3.8	4.6	5.13
sc	20.9	3.324	8.482	6.227	1.289	3.8	4.6	–
pc	21.0	3.330	8.317	6.189	1.274	3.9	4.7	5.13
	20.3	3.588	9.715	7.372	1.950	3.6	4.1	–
	20.3	3.588	9.762	7.414	1.972	3.6	4.1	4.20
sc	20.4	3.619	9.914	7.471	2.020	3.6	4.1	4.18
	20.2	3.581	9.847	6.738	1.626	3.8	4.4	4.16
	20.2	3.582	9.692	6.729	1.622	3.8	4.4	4.30
	20.2	3.584	9.692	6.723	1.620	3.8	4.4	4.54
	20.2	3.579	9.661	6.736	1.624	3.8	4.4	4.43
	20.2	3.582	9.692	6.776	1.640	3.8	4.4	4.28
	20.2	3.580	9.691	6.727	1.620	3.8	4.4	4.50
	20.4	3.986	10.847	7.950	2.519	3.7	4.1	–
	20.4	3.986	10.885	7.986	2.542	3.7	4.1	4.27
	20.4	3.986	10.888	7.920	2.500	3.7	4.1	–
	20.4	3.972	10.845	7.967	2.521	3.7	4.1	3.98
	20.4	3.986	10.890	7.999	2.551	3.6	4.0	4.19
	20.0	2.649	6.047	3.778	0.378	4.7	7.3	6.42
	20.0	2.649	6.066	3.773	0.377	4.7	7.4	6.50

o Twin Sisters dunite; sc and pc refer, respectively, to gem-quality single-crystals and synthetic polycrystalline aggregates. The single-cr
t-Reuss-Hill (VRH) values in all cases.

Then taking the first derivative with respect to pressure, we have

$$\left(\frac{\partial K_s}{\partial p}\right)_s = \left(\frac{\partial \rho}{\partial p}\right)_s (a + b\rho)^2 + 2b\rho\,(a + b\rho)\left(\frac{\partial \rho}{\partial p}\right)_s .$$

Since the bulk modulus is given by $K_s \equiv \rho\,(\partial p/\partial \rho)_s$, we can obtain from eqs. (2) and (3) that

$$\left(\frac{\partial K_s}{\partial p}\right)_s = 1 + \frac{2b\rho}{V_\phi} = 1 + 2b\rho\,(\rho/K_s)^{\frac{1}{2}} \qquad (4)$$

By using $b = 2.65$ (km/sec)/(g/cm^3) *, the author tested in table 1 the compatibility of eq. (4) with experimental $(\partial K_s/\partial p)_T$ values for all those oxides and silicates about the mean atomic weight of 20 to 21, which have been determined in recent years by ultrasonic methods. In all cases, the calculated $(\partial K_s/\partial p)_s$ values are smaller than the experimental $(\partial K_s/\partial p)_T$ values determined on the same material; the calculated values, relative to the measured $(\partial K_s/\partial p)_T$, were about 27% smaller for quartz, about 26% smaller for olivine, about 15% smaller for spinel, about 13% smaller for periclase and about 12% smaller for corundum. The greater the bulk modulus of material, the smaller the difference between the measured and calculated values of $(\partial K_s/\partial p)$. Thus, a correction term (C/K_s) to eq. (4) is necessary; it arises from our observation that the difference between the measured and calculated values of $(\partial K_s/\partial p)$ is inversely proportional to the bulk modulus of material. Rewriting eq. (4) with this correction term, we have then

$$\left(\frac{\partial K_s}{\partial p}\right)_s \simeq 1 + \frac{2b\rho}{V_\phi} + \frac{C}{K_s}, \qquad (5)$$

where, to the first-order approximation, C is one in the same units of K_s (in Mb). Thus, the effect of the correction term (C/K_s) on $(\partial K_s/\partial p)_s$ is large for materials of small K_s, but for materials of large K_s the correction becomes relatively small. Using eq. (5), $(\partial K_s/\partial p)_s$ for quartz, olivine, periclase, spinel and corundum are newly calculated; the calculated $(\partial K_s/\partial p)_s$ values for these materials are, respectively, 7.3, 4.6, 4.4, 4.1 and 4.1 and these values compare favorably with experimental $(\partial K_s/\partial p)_T$ values of 6.5 (±0.3), 5.0 (±0.3), 4.3 (±0.2), 4.3 (±0.3), and 4.2 (±0.2) as reported in the literature [5, 6]. It is then seen that eq. (5) could be used for estimating the value of $(\partial K_s/\partial p)_s$ for crystalline solids for which ultrasonic-pressure experiments are limited by the present state of technology involving material synthesis and characterization.

The usefulness of eq. (5), and also the thought behind it, is apparent since the quantities like b, V_ϕ, ρ and K_s can be obtained readily as outlined in earlier paragraphs. Rigorously speaking, the parameter $(\partial K/\partial p)$ enters into equations describing the pressure-volume relationships in solids. The difference arising from thermodynamic corrections as detailed elsewhere [7] between the $(\partial K_s/\partial p)_s$ value resulting from eq. (5) and $(\partial K/\partial p)_T$ or that between the experimental $(\partial K_s/\partial p)_T$ and the calculated $(\partial K_s/\partial p)_s$ is about 1–2% each. For all practical purposes in geophysics, these corrections can be ignored and we use the $(\partial K_s/\partial p)_s$ values in the following discussion.

3. Illustration of the scheme

Some examples for illustrating the use of eqs. (3) and (5) follow. The first example is concerned with finding the equations of state for the spinel phase formed under pressure from the olivine structure in the $(Mg, Fe)_2 SiO_4$ system. In table 2 (part A), the density ρ and the bulk sound velocity V_ϕ of olivine-transformed spinels are tabulated. From these ρ and V_ϕ values, K_s and $(\partial K_s/\partial p)_s$ are calculated according to eqs. (3) and (5), respectively; the results are entered in the table for three $(Mg_x Fe_{1-x})_2 SiO_4$-spinels. Using these EOS parameters, the volume-pressure trajectories inferred from the Birch equation of state [1] are shown in fig. 1 for olivines and the olivine-transformed spinels. Superimposed on this figure are the data points resulting from isothermal compression experiments by Mao et al. [8] for three iron-rich spinels transformed under pressure from their respective olivine structures. It is clearly seen in fig. 1 that, although the present comparison is made for a pressure range of about 15% of the bulk modulus, there is strong

* Based on the ultrasonic velocity data in table 1, the V_ϕ values of 35 data points for 22 substances (whose mean atomic weights range from 20 to 21) are fitted to eq. (2) by a least squares method. The coefficients in eq. (2) are found to be $a = -2.59$ (km/sec) and $b = 2.65$ (km/sec)/(g/cm^3); the correlation coefficient is 0.96 and the standard error is 0.14 (km/sec). This value of b is in good agreement with $b = 2.59$ (km/sec)/(g/cm^3) found earlier by Wang [4].

Table 2
Equation of state parameters of olivine-transformed spinels, coesite and stishovite of silica polymorphs and the possible high-pressure phases of pyroxene.

High-pressure phase	Density (g/cm^3)	V_ϕ (km/sec)	K_s (Mb)	$\frac{\partial K_s}{\partial p}$
Part A:				
β-Mg_2SiO_4	3.556	7.24	1.86	4.1
γ-$(Mg, Fe)_2SiO_4$	3.800	6.78	1.93	4.8
γ-Fe_2SiO_4	4.849	6.35	1.96	5.5
Part B:				
Coesite	2.920	4.70	0.65	5.8
Stishovite	4.287	9.8	4.1	3.4
Part C:				
(1) Garnet	3.64	6.55	1.56	4.6
(2) Spinel + stishovite	3.77	6.82	1.75	4.5
(3) Ilmenite	3.85	7.08	1.91	4.3
(4) Oxides-mixture	4.08	7.50	2.32	4.2
(5) Perovskite	4.35	8.10	2.83	4.1
Estimated uncertainty %	0.5	5	5	10

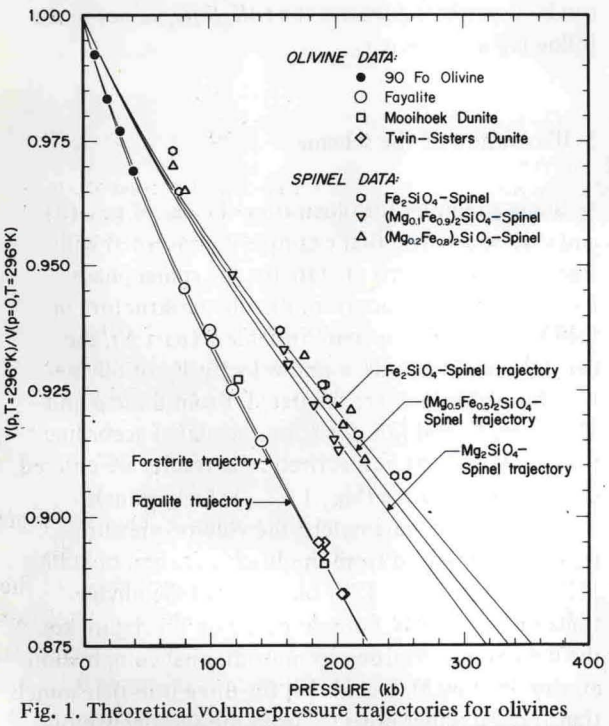

Fig. 1. Theoretical volume-pressure trajectories for olivines and olivine-transformed spinels; comparison with isothermal compression data. The solid lines are the results of the present theory, and they are independent of the compression data points.

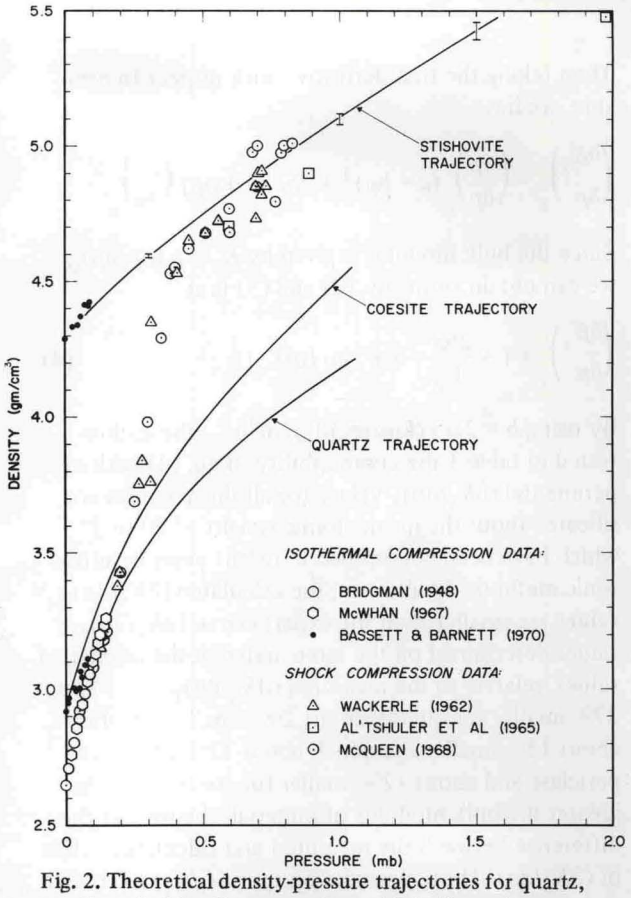

Fig. 2. Theoretical density-pressure trajectories for quartz, coesite and stishovite; comparison with isothermal compression data and shock-wave data points. The solid lines are the results of the present theory and they are independent of the compression data points.

evidence of agreement between the theoretical volume-pressure trajectories and the experimental compression data for the olivine-transformed spinels.

The second example deals with the equations of state of silica polymorphs under pressure. Quartz, stable at ambient conditions, transforms to coesite at about 20 kb pressure and then to stishovite at pressures above 90 kb. With the use of the scheme proposed here, the author finds the EOS parameters of coesite and stishovite as tabulated in table 2 (part B). As in the first example with spinels, the density-pressure trajectories resulting from the Birch equation of state with the parameters listed in table 2 (Part B) are shown in fig. 2. Superimposed on this figure with these trajectories are isothermal compression data points of Bridgman [9], McWhan [10], and Bassett and Barnett [11] for quartz, coesite and stishovite phases, respectively. Also superimposed on the present density-pres-

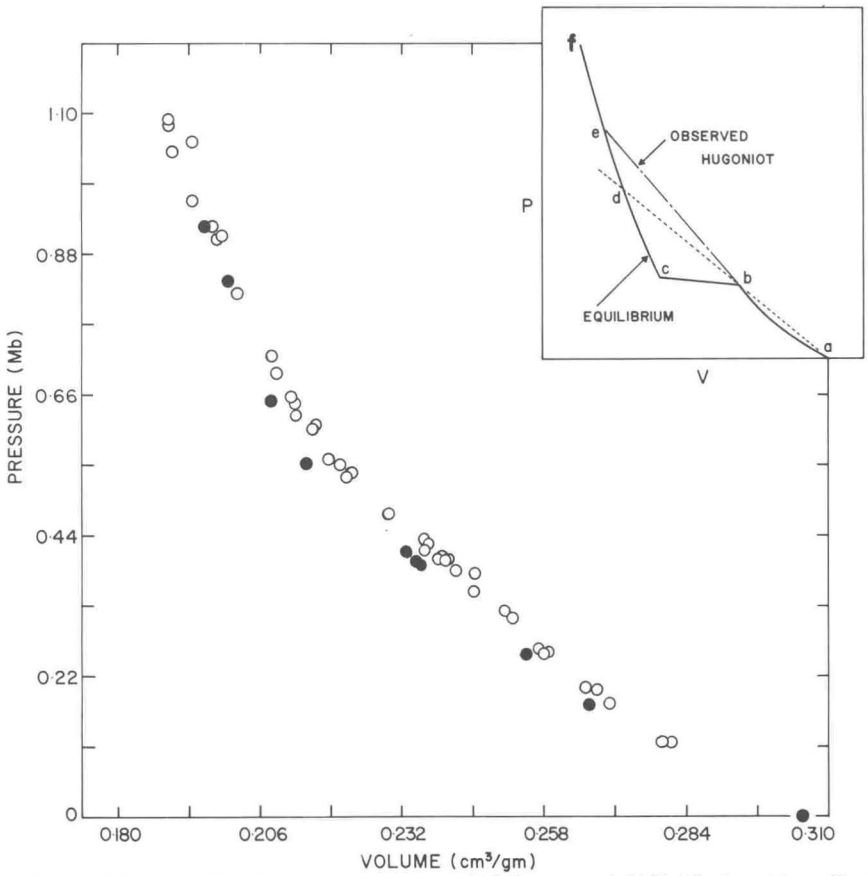

Fig. 3. Display of shock-wave data points for a bronzititic pyroxene of McQueen et al. [15]. The insert is an illustration of a pressure-volume Hugoniot of a solid undergoing phase change. The equilibrium pressure-volume relation is given by the path abcf. Under most shock conditions, the solid-solid transformation begins immediately but does not go to completion; the pressure-volume relation in this case follows a path designated by abef.

sure trajectories are those data points resulting from shock-wave compression experiments of Wackerle [12], Al'tshuler et al. [13] and McQueen [14]. The present trajectory for stishovite, with possible errors as indicated in fig. 2, is seen to match the shock-wave data points in the high-pressure region quite well.

The third example is concerned with an application of the present scheme for a study of high-pressure phases in the earth's interior. Pyroxene, next to olivine, is believed to be one of the most abundant minerals in the upper mantle. Pyroxene subjected to mantle conditions undergoes a number of phase changes. Much of the geophysical literature [17] suggests that pyroxene, with a composition of $(Mg_{0.9}\,Fe_{0.1})SiO_3$ for example, would transform to 1) garnet, 2) spinel plus stishovite, 3) ilmenite, 4) a mixture of close-packed oxides (referred to hereafter as "oxidesmixture") and/or 5) perovskite structure. The use of eqs. (3) and (5), when combined with shock-wave compression data, can permit one to conclude which of these phases is most probable at high pressures. Take the example as follows.

Consider the compression data resulting from shock-wave experiments on a bronzititic pyroxene as displayed in fig. 3. These data on bronzititic rocks of the Bushveld and Stillwater Complexes are from McQueen et al. [15]. These rocks are characterized by high-purity orthopyroxene with an Fe/Mg ratio of about 0.1. Under most shock conditions, the solid-solid transformation begins immediately but does not go to completion; this means that, although the pressure lies slightly above the Raleigh ray through the "mixed-phase"

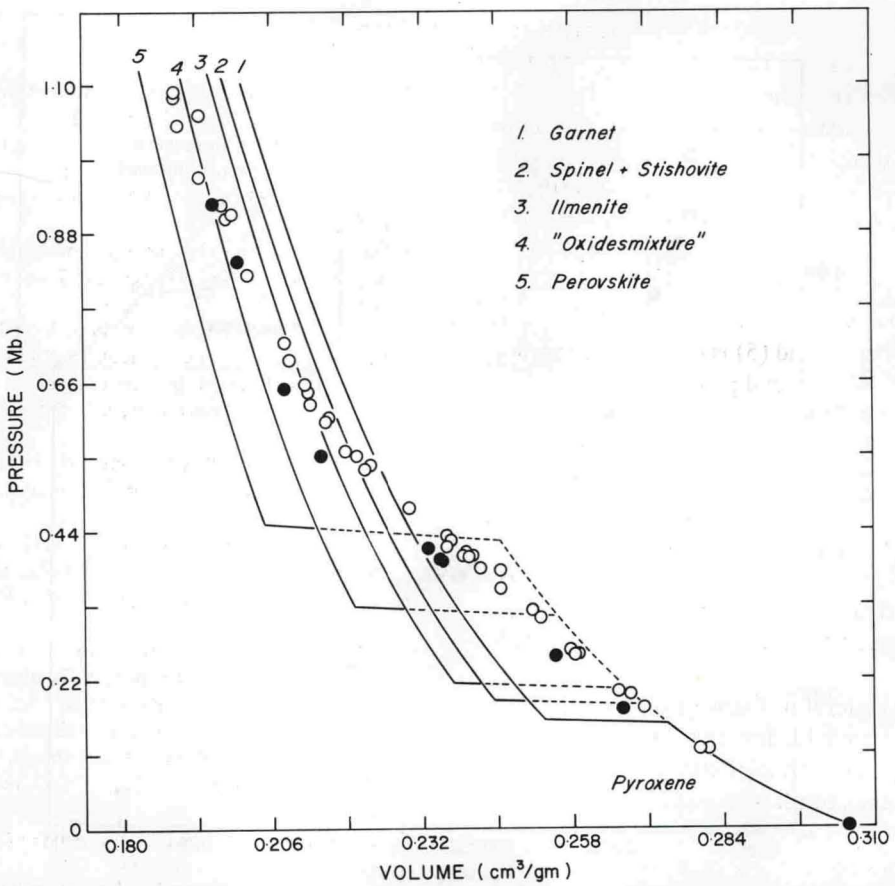

Fig. 4. Analysis of the shock-wave data points displayed in fig. 3 in terms of the possible high-pressure phases of pyroxene. The most probable high-pressure phase of bronzititic pyroxene is *"oxidesmixture"*, as illustrated by the pressure-volume Hugoniot (4) at high pressures.

region as illustrated by the insert in fig. 3, the slope does not increase as rapidly as it would if the material had stayed in the initial phase. Therefore, the data points as displayed in this figure constitute a series of pressure-volume relationships for different phases in metastable conditions. Analysis of these data points would then be possible only for two regions of pressures, one at low pressures where bronzitite is stable and the other at high pressures where this material transformed to the most stable high-pressure phase. The EOS parameters of pyroxene with this bronzitite composition ($\rho_0 = 3.273$ g/cm^3) have been reported by this author [16] as $K_s = 1.06$ (±0.03) Mb and $(\partial K_s/\partial p) = 5.5$ (±0.3). Based on these parameters and using the scheme in this paper (as illustrated by the two examples above), we can find K_s and $(\partial K_s/\partial p)$ values for all possible high-pressure phases listed earlier from eqs. (3) and (5). Results of these calculations are summarized in table 2 (part C). The pressure-volume trajectories * inferred from the usual Hugoniot equation of state [15] are shown in fig. 4; superimposed on these trajectories are those shock-wave data presented in fig. 3. Note that, at low pressures, the pressure-volume trajectory of pyroxene superimposes well on the low-pressure shock compression data. Note also that trajectory (4), labelled *oxidesmixture*, matches the compression data points in the 0.8–1.1 Mb region very well, suggesting that the most stable phase of the bronzitite under high pressures is the *oxidesmixture* of (x periclase + y wüstite + z

* Footnote: See next page.

stishovite) which has a mean density at zero pressure $\bar{\rho}_0$ of 4.08 g/cm^3. This value of $\bar{\rho}_0$ compares very well with 4.10 (±0.05) g/cm^3, the density value obtained by extrapolation of trajectory (4) to the zero-pressure point by the use of the Birch equation of state. Thus, the usefulness of the proposed scheme for identification of phases and their densities at high pressures is readily observed.

In summary, then, the author concludes the following: a) the analytical scheme proposed in this paper involving eqs. (3) and (5) is useful for constructing equations of state of solid phases that cannot be determined experimentally given the present state of technology, and b) one now should be able to model in the laboratory the elasticity and constitution of the earth's interior by incorporating the information on experimental petrology, high-pressure compression data and geophysical field observations in this approximation scheme. In a subsequent series of communications, the results of such an attempt shall be reported.

The author is grateful to Francis Birch who gave encouragement to look further into the equations of state of high-pressure solid phases. The idea presented here is simple, but it works as illustrated, and it is the only one of its kind proposed in the geophysical literature. This study was supported by the National Science Foundation.

* The Hugoniot curve is found from the pressure-volume-energy (PVE) surface specified by the input through the constraint equation

$$E_2 - E_1 = \tfrac{1}{2}(p_1 + p_2)(V_1 - V_2)$$

which is the energy-jump condition for a shock transition from State 1 to State 2. In the case of a phase transition, the Gibbs free energy is found by integrating the equation of state of each phase and the additional constraint that "the Gibbs free energy must be equal" is imposed in the mixed-phase region. The slope of the equilibrium Hugoniot curve in the mixed-phase region depends on the entropy difference and volume difference between phases. For any reasonable value of these parameters, the slope of the equilibrium Hugoniot curve in the mixed-phase region is much smaller than the slope of the actual shock-wave data points. Therefore, the transition does not go to completion in the shock experiments and in this intermediate region consisting of mixed phases no conclusion on density of the high-pressure phase can be drawn.

References

[1] F. Birch, Elasticity and constitution of the earth's interior, J. Geophys. Res. 57 (1952) 227.

[2] F. Birch, Composition of the earth's mantle, Geophys. J. Roy. Astron. Soc. 4 (1961) 295;
D.H. Chung, Birch's law: Why is it so good? Science 177 (1972) 261.

[3] D.H. Chung, Elasticity and equations of state of olivines in the Mg_2SiO_4-Fe_2SiO_4 system, Geophys. J. Roy. Astron. Soc. 25 (1971) 511;
Effects of iron/magnesium ratio on P- and S-wave velocities in olivine, J. Geophys. Res. 75 (1970) 7353.

[4] C.Y. Wang, Equation of state of periclase and some of its geophysical implications, J. Geophys. Res. 74 (1969) 1451;
R.G. McQueen, S.P. Marsh and J.N. Fritz, On the composition of the earth's interior, J. Geophys. Res. 69 (1964) 2947.

[5] O.L. Anderson, E. Schreiber, R.C. Liebermann and N. Soga, Some elastic constant data on minerals relevant to geophysics, Rev. Geophys. 6 (1968) 491; for discussion, see ref. [6].

[6] D.H. Chung, Pressure coefficients of elastic constants for porous materials: Correction for porosity and discussion on literature data, Earth Planet. Sci. Letters 10 (1971) 316. In table 4 on page 322 and in the text, the porosity-corrected hematite data should have been $(d\mu^\circ/dp) = 0.73$ and $(dK_S^\circ/dp) = 4.57$, *not* 0.89 and 4.91.

[7] D.H. Chung, First pressure derivatives of polycrystalline elastic moduli: Their relation to single-crystal acoustic data and thermodynamic relations, J. Appl. Phys. 38 (1967) 5104.

[8] H. Mao, T. Takahashi, W.A. Bassett, J.S. Weaver and S. Akimoto, Effect of pressure and temperature on the molar volumes of wüstite and of three $(Fe, Mg)_2SiO_4$-spinel solid solutions, J. Geophys. Res. 74 (1969) 1061.

[9] P.W. Bridgman, The compression of 39 substances to 100,000 kg/cm^2, Proc. Am. Acad. Arts & Sci. 76 (1948) 55.

[10] D.B. McWhan, Linear compression of α-quartz to 150 kbar, J. Appl. Phys. 38 (1967) 347.

[11] W.A. Bassett and J.D. Barnett, Isothermal compression of stishovite and coesite to 85 kbars at room temperature by X-ray diffraction, Phys. Earth Planet. Interiors 3 (1970) 54.

[12] J. Wackerle, Shock-wave compression of quartz, J. Appl. Phys. 33 (1962) 822.

[13] L. V. Al'tshuler, R.F. Truinin and G.V. Simakov, Shock-wave compression of periclase and quartz and compression of the earth's lower mantle, Phys. Solid Earth 10 (1965) 657.

[14] R.G. McQueen, Sock-wave data and equations of state, in Seismic Coupling, ed. G. Simmons (Univ. Michigan Geophys. Lab. Publ., Ann Arbor 1968).

[15] R.G. McQueen, S.P. Marsh and J.N. Fritz, Hugoniot equation of state of 12 rocks, J. Geophys. Res. 72 (1967) 4999.
[16] D.H. Chung, Equations of state of pyroxenes in the $MgSiO_3$-$FeSiO_3$ system, Trans. Am. Geophys. Union 52 (1971) 919.
[17] A.E. Ringwood, Phase transformation in the mantle, Earth Planet. Sci. Letters 5 (1969) 401.

References to table 1:

[18] F. Birch, The velocity of compressional waves in rocks to 10 kilobars, Part 1, J. Geophys. Res. 65 (1960) 1083; Part 2, J. Geophys. Res. 66 (1961) 2199.
[19] G. Simmons, The velocity of shear waves in rocks to 10 kilobars, J. Geophys. Res. 69 (1964) 1123.
[20] G. Simmons and A.W. England, Universal equations of state for oxides and silicates, Phys. Earth Planet. Interiors, 3 (1969) 69.
[21] M. Kumazawa, The elastic constants of single-crystal orthopyroxene, J. Geophys. Res. 74 (1969) 5973.
[22] T.V. Ryzhova, K.S. Alexandrov and V.M. Korobkova, The elastic properties of rock-forming minerals; 5. Additional data on silicates, Izv. Acad. Sci. USSR, Phys. Solid Earth 2 (1966) 111.
[23] M. Kumazawa and O.L. Anderson, Elastic moduli, pressure derivatives, and temperature derivatives of single-crystal olivine and single-crystal forsterite, J. Geophys. Res. 74 (1969) 5961.
The inversion procedure described in this paper, on page 5968 and thereafter, is incorrect. The equation, for example, given by these authors on mid-page 5968 is

$$\frac{dS_{ij}}{dX} = \frac{1}{\Delta_0}\left[A_{ij} - S_{ij0}\Delta\right]$$

and this equation is dimensionally inconsistent. The correct equation should have been

$$\frac{d\hat{S}}{dX} = -\hat{S}\frac{dC}{dX}\hat{S}.$$

[24] H. Mizutani, Y. Hamano, Y. Ida and S. Akimoto, Compressional wave velocities in fayalite, Fe_2SiO_4-spinel, and coesite, J. Geophys. Res. 75 (1970) 2741.
[25] R.K. Verma, Elasticity of some high density crystals, J. Geophys. Res. 65 (1960) 757.
[26] M.F. Lewis, Elastic constants of magnesium aluminate spinel, J. Acoust. Soc. Am. 40 (1966) 729.
[27] D.H. Chung, Equations of state of olivine-transformed spinel, Earth Planet. Sci. Letters 14 (1972) 348.
[28] E. Schreiber, Elastic moduli of single-crystal spinel at 25°C and to 2 kbar, J. Appl. Phys. 38 (1967) 2508.
[29] E.H. Bogardus, Third-order elastic constants of Ge, MgO, and fused SiO_2, J. Appl. Phys. 36 (1965) 2504.
[30] D.H. Chung and W.R. Buessum, The Voigt-Reuss-Hill (VRH) approximation and the elastic moduli of polycrystalline MgO, CaF_2, β-ZnS, ZnSe, and CdTe, J. Appl. Phys. 38 (1967) 2535.
[31] D.H. Chung and G. Simmons, Elastic properties of polycrystalline periclase, J. Geophys. Res. 74 (1969) 2133.
[32] H. Spetzler, Equation of state of polycrystalline and single-crystal MgO to 8 kbar and 800°K, J. Geophys. Res. 75 (1970) 2073.
[33] J.B. Wachtman, Jr., W.E. Tefft, D.G. Lam Jr. and R.P. Stinchfield, Elastic constants of synthetic single-crystal corundum at room temperature, J. Res. NBS (U.S.A.) 64A (1960) 213.
[34] J.H. Gieske and G.R. Barsch, Pressure dependence of the elastic constants of single-crystal aluminum oxide, Phys. Status Solidi 29 (1968) 121.
[35] D.H. Chung and W.R. Buessem, The VRH approximation and the elastic moduli of polycrystalline ZnO, TiO_2 and α-Al_2O_3, J. Appl. Phys. 39 (1968) 2777.
[36] D.H. Chung and G. Simmons, Pressure and temperature dependences of the isotropic elastic moduli of polycrystalline alumina, J. Appl. Phys. 39 (1968) 5316.
[37] H.J. McSkimin, P. Andreatch and R.W. Thurston, Elastic moduli of quartz versus hydrostatic pressure at 25°C and −195.8°C, J. Appl. Phys. 36 (1965) 1624.
[38] D.H. Chung and G. Simmons, Pressure derivatives of the elastic properties of polycrystalline quartz and rutile, Earth Planet. Sci. Letters 6 (1969) 134.